

Emission Kinetics from PbSe Quantum Dots in Glass Matrix at High Excitation Levels

Jin Hong, Han Wang, Fangyu Yue,* Jens W. Tomm,* Detlef Kruschke, Chengbin Jing, Shaoqiang Chen, Ye Chen, Weida Hu, and Junhao Chu

The photoluminescence dynamics of PbSe quantum dots in a glass matrix (PbSe:Glass) is investigated at high excitation levels. Up to 470 meV blue-shifted emissions are observed, which are assigned to excited-state emission populated by carrier accumulation. Rapid photoluminescence decays of $\sim 25\text{--}40$ ps are observed. Together with a threshold-like dependence on excitation, even at room temperature, this component is tentatively attributed to amplified spontaneous emission. The absence of stimulated emission from the ground state and the overall higher threshold compared to PbS:Glass suggest that there are more intrinsic restrictions on the use of PbSe:Glass as a laser material than for PbS:Glass.

- the eightfold degeneracy (including spin) of the lowest-quantized states that directly impacts the optical gain, and intrinsically limits stimulated emission;
- the presumably high Auger recombination rate in narrow-gap Pb-salts can severely limit lifetimes of e-h pairs states that are responsible for optical gain^[9,10]; and
- practically, the low volume fraction (f) of QDs in glass matrix limits its application to lasers.

Lead salt quantum dots (QDs) are interesting materials for potential applications as lasing media due to the wide tuning of the fundamental optical resonance energy from the mid-infrared to the visible.^[1] Among the binary lead salts, PbSe takes a special role, as it has the smallest bandgap (E_g)-value of 0.27 eV only, the smallest effective mass(es) of $m_e \approx m_h \approx 0.061 m_0$, and the largest Bohr radius of 46 nm.^[2,3] This promises well pronounced quantum-size effects and an excitonic fine structure with intraband energy spacings significantly larger than phonon energies.^[4,5] In contrast to colloidal hosts, glass matrices (QD:Glass) provide substantial advantages including capability, stability, and robustness. These assets make QD:Glass systems, e.g., PbSe:Glass, a highly desirable candidate as gain material.^[6]

Within the two decades of their existence as research topic, however, QD:Glass including PbSe:Glass haven't made it to commercial applications.^[7,8] Discouraging facts are:

Nevertheless, amplified spontaneous emission (ASE) and optical gain based on PbSe QDs (sol-gel thin films or fiber structures) have been observed or predicted for ground-state emission.^[11–13] More important, even stimulated emission was revealed in PbS:Glass with a relatively low f -value of 0.025%.^[14] These reports suggest that the natural limitation of Pb-salt QDs for lasing application can be experimentally overcome, and PbSe:Glass with stronger quantum-confinement and elevated f -values could be suitable as lasing material, provided that the mechanisms leading to stimulated emission in QD:Glass can be addressed. Therefore, from the point of view of laser application, it is important to re-consider the pro and cons of this potentially utmost interesting class of photonic material, and to update, if available, new arguments to one of these two contradictory sides.

In this paper, we report on time-resolved photoluminescence (PL) of PbSe:Glass at optical excitation levels of up to

J. Hong, H. Wang, Prof. F. Yue, Prof. C. Jing, Prof. S. Chen, Prof. Y. Chen, Prof. J. Chu
Key Laboratory of Polar Materials and Devices
Ministry of Education
East China Normal University
200241 Shanghai, P.R. China
E-mail: fyyue@ee.ecnu.edu.cn

Dr. J. W. Tomm
Max-Born-Institut für Nichtlineare Optik und Kurzzeitspektroskopie
Max-Born-Str. 2A
12489 Berlin, Germany
E-mail: tomm@mbi-berlin.de

Dr. D. Kruschke
Institut für Angewandte Photonik e.V.
Rudower Chaussee 29/31
12489 Berlin, Germany

Prof. W. Hu, Prof. J. Chu
National Laboratory for Infrared Physics
Shanghai Institute of Technical Physics
Chinese Academy of Sciences
200083 Shanghai, P.R. China

 The ORCID identification number(s) for the author(s) of this article can be found under <https://doi.org/10.1002/pssr.201800012>.

DOI: 10.1002/pssr.201800012

$50 \mu\text{J} \cdot \text{cm}^{-2}$ per pulse. Instead of the excitonic ground state emission, which is observed at low excitation levels with a PL decay time on the order of μs , at least two fast emission contributions are observed energetically blue-shifted by up to 0.47 eV. For them, the initial PL decay time constant is $\sim 25\text{--}40$ ps. They are attributed to excited state emission. The presence of a superlinear increase in emission with a threshold of $\sim 20 \mu\text{J} \cdot \text{cm}^{-2}$ indicates the beginning of ASE. However, the absence of any emission from the ground state and a significantly higher threshold value compared to PbS:Glass indicate a worse potential of PbSe:Glass as a gain medium compared to PbS:Glass.

Materials and Methods: PbSe:Glass samples were grown according to the method introduced by Borrelli.^[15] Plate 3.5 mm in thickness were cut and subsequently annealed in two steps: $475^\circ\text{C}/20\text{ h} + 535^\circ\text{C}/1\text{ h}$.^[16] Sample lamellas are prepared by polishing both sides. Thicknesses are between $150 \mu\text{m}$ to 3 mm. A Fourier transform infrared (FTIR) spectrometer is employed for the absorption and steady-state PL (SS-PL) characterization, and a time-resolved PL (TR-PL) system is employed for monitoring the fast PL process (see Supporting Information for details).

Results: Figure 1a shows absorption and SS-PL spectra, excited with cw-514 nm laser, from a 0.5-mm thick sample at 300 K. The excitonic ground-state resonance energy (for simplicity, from now on called E_g) is at 0.951 eV as concordantly determined by Gaussian- and the second-order derivative-fits.^[17–19] According to the hyperbolic-band model,^[20] the average diameter of the

QDs is 3.4 nm, consistent with the value of (3.3 ± 0.3) nm (the variation in size $\approx 9\%$) as obtained from TEM; see insets in Figure 1a. Thus, the volume fraction of the QDs in the glass matrix is $f \approx 0.07\%$, pointing to 5×10^{16} QDs cm^{-3} . This is close to the value obtained from the absorption coefficient at 400 nm.^[21] The variation in size is less than 5% referring to the full width at half maximum (FWHM) of the ground-state absorption peak measured at various temperatures.^[22] The PL spectrum can be fit with a single-Gaussian function that is centered at 0.895 eV (for simplicity, called E_g'). This points to a Stokes shift of 56 meV at 300 K.

Figure 1b shows the temperature dependencies of PL and absorption peaks. Obviously, the energetic difference between them, the Stokes shift, substantially decreases toward ambient temperature. These data allow deriving standard characteristics of the QDs by employing semi-empirical expressions.^[23–25] We find a temperature coefficient $dE_g'/dT = (120 \pm 9) \mu\text{eV K}^{-1}$, and Debye temperature of (101 ± 19) K. The longitudinal optical (LO) phonon energy (18.6 ± 2.6) meV is consistent with reports,^[26,27] but falls below the value of (29.6 ± 0.8) meV obtained from the FWHM(T) evolution. The Arrhenius plot of the PL line points to an activation energy of 16.5 meV, see inset in Figure 1b, which matches the LO phonon energy obtained from the $E_g'(T)$ evolution. Figure 1c completes the sample characterization by providing excitation dependencies of PL signal, peak energy, and FWHM. The weak excitation dependencies of E_g' and FWHMs together with the slope of unity of the PL (integral) intensity across an excitation range of two orders of magnitude, clearly indicate ground-state emission without any alterations of the PL line shape in the entire excitation range.

Figure 1d gives typical PL decay curves at 5 and 300 K at low excitation densities (ns-pulsed excitation at 1064 nm), where substantially less than one electron-hole-pair per QD is generated. The single-exponential decay function fit reveals a μs lifetime of the E_g' -related non-equilibrium carriers, about one order of magnitude longer than sub- μs of colloidal systems.^[4,28]

After the basic characterization of structural and optical properties of samples, we precede to high excitation levels by using the TR-PL system. Figure 2a–c show exemplary original transient PL data matrixes as monitored by the system. The most striking feature in Figure 2 is the presence of two emission bands (labelled A and B) even at reduced excitation density; see Figure 2a, and ambient temperature; see Figure 2c. Both bands include a fast (\sim ps) and a slow (\sim ns) process. Notice that the high repetition rate (≈ 12.5 ns between two subsequent pulses is more than two orders of magnitude shorter than that of the μs time constant of the excitonic ground-state. In concert with this special excitation condition, the μs time constant gives rise to a background signal, i.e., an accumulated PL contribution at probe time $t < 0$. In the following, this background will be called I_0 . Figure 2d shows the time-integrated data given in Figure 2b together with SS-PL and absorption spectra taken at 5 K. Notice that the two emission bands at $E_A \approx 1.13$ eV, $E_B \approx 1.32$ eV are blue-shifted by 280 and 470 meV, respectively, with regard to the SS-PL peak ($E_g' \approx 0.85$ eV).

It is worth to mention that both bands are not detectable in any steady-state experiments including other excitation wavelengths, e.g., 405 nm, and also not for ns-pulsed excitations or fs-pulsed excitations with a repetition rate of 250 kHz, suggesting that:

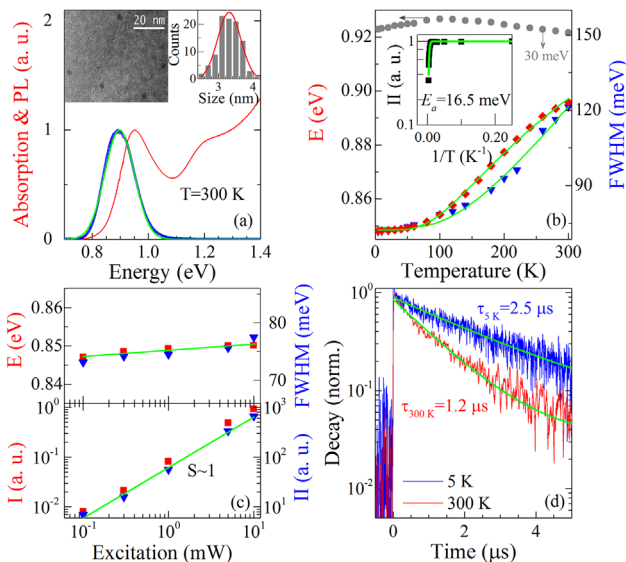


Figure 1. Standard characterization of the PbSe:Glass sample. a) Absorption and SS-PL spectra at 300 K. The insets give TEM images of a lamella with five QDs and a size distribution of QDs taken from several lamellas fitted by a Gaussian. b) Temperature dependencies of PL peak energy and FWHM, and the absorption peak energy (gray; downshift by 30 meV). The inset shows an Arrhenius plot of the integrated PL signals. c) Excitation dependencies of PL peak energy and FWHM (top), and PL peak intensity and integrated intensity (bottom). d) Decay curves and decay function fits for 5 K and 300 K. All solid lines in green in subfigures are fit results.

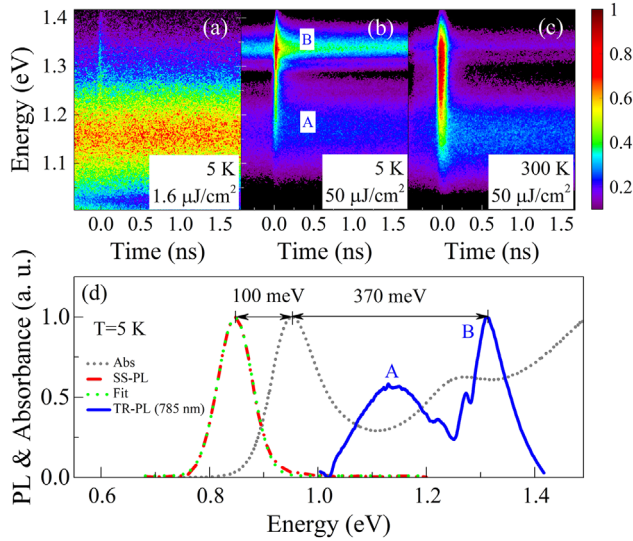


Figure 2. Normalized original PL data matrices at high excitation levels: (a) 5 K, $1.6 \mu\text{J} \cdot \text{cm}^{-2}$; (b) 5 K, $50 \mu\text{J} \cdot \text{cm}^{-2}$; (c) 300 K, $50 \mu\text{J} \cdot \text{cm}^{-2}$. d) Overview on the PL behavior: Time-integrated spectrum from (b) together with SS-PL and absorption spectra, all taken at 5 K.

- the carrier accumulation due to the high repetition rate of 80 MHz of the fs laser plays a main role in generation of these emission bands, and
- these blue-shifted emissions do not originate from the ground-state, but from higher levels, such as excited states.

Figure 3a shows the PL spectra taken as vertical cuts from matrices as shown in Figure 2b. The two emission bands A and B are well-pronounced at the beginning of the pulse, and become clearly separated after 1.5 ns. Figure 3b gives the PL transients taken as horizontal cuts out of matrixes. Both emission bands show non-exponential decays with a common shape including a faster (τ_f) and slower (τ_s) decay component, as well as the accumulated background I_0 . The transient can be fitted by a double-exponential decay function plus a tail (I_t). At an excitation of $50 \mu\text{J} \cdot \text{cm}^{-2}$, the fit procedures give two time constants: $\tau_{Af} \approx 40 \text{ ps}$ and $\tau_{As} \approx 1.5 \text{ ns}$ for band A, and $\tau_{Bf} \approx 25 \text{ ps}$ and $\tau_{Bs} \approx 180 \text{ ps}$ for band B.

Figure 3c shows the PL decay curves of peak A at different excitation densities. With increasing excitation, a fast component emerges. The slow component resembles the behavior of spontaneous emission, and is characterized by I_0 . Its time constant of $\sim 1.5 \text{ ns}$, about three orders of magnitude faster than the μs lifetime of the excitonic ground-state emission, see Figure 1d, also matches the expected non-equilibrium carrier lifetime of excited states in such materials.^[29,30]

It is vital to point out that the I_0 shows a slope of unity versus excitation ($S \approx 1.0$); see the inset in Figure 3d. This suggests that despite the carrier accumulation, non-linear non-radiative recombination, e.g., Auger recombination, is still not effective. Notice that the maximum photon fluency density per pulse ($5 \times 10^{15} \text{ cm}^{-3}$ based on the experimental value $\alpha(785 \text{ nm}) \approx 10 \text{ cm}^{-1}$) is one order of magnitude smaller than the density of QDs, $5 \times 10^{16} \text{ cm}^{-3}$. Moreover, the excitation energy $E_{ex} = 1.58$

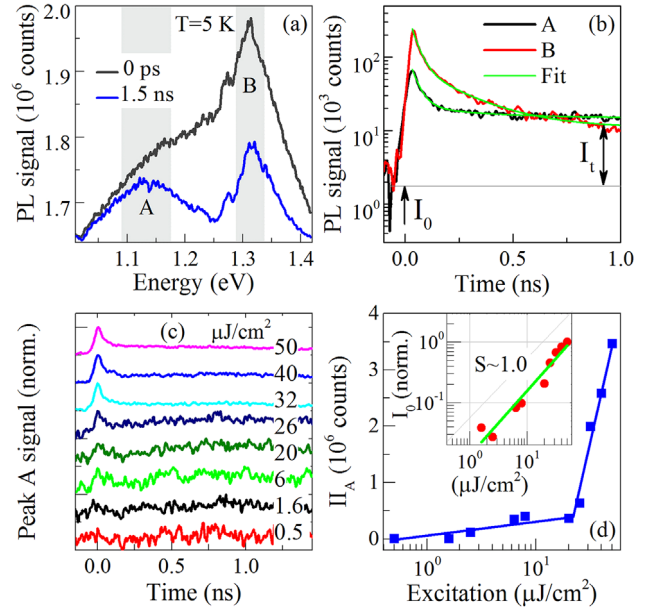


Figure 3. a) PL spectra taken from the matrix in Figure 2b at 0 ps and 1.5 ns at 5 K. b) PL transients and fits for peak A (1.13 eV) and peak B (1.32 eV). c) Decay curves of peak A at different excitation densities. d) Excitation dependence of the integral intensity of peak A taken from decay curves. The solid line in blue is a guide to the eyes. The inset gives the excitation dependence of the normalized I_0 , where the solid line in green is the linear-fit result.

$\text{eV} \approx 1.6 \times E_g$ is substantially smaller than double of all emission peak energies including E_A and the following E_B , which should exclude the effect of multiple exciton generation.^[31,32] Even more important,

- the integral intensity of the fast component depends in a superlinear way on excitation, as shown in Figure 3d, which shows a threshold-like excitation value at $20 \mu\text{J} \cdot \text{cm}^{-2}$; and
- the fast component shows no dependencies of excitation, and even temperature,
- therefore, the fast component with a typical decay time of $\sim 40 \text{ ps}$ could account for amplified spontaneous emission (ASE). This is consistent with the observation of stimulated emission in PbS:Glass material system.^[14,33,34]

We should emphasize that our assignment to ASE is not a claim about the presence of lasing, but just an indication that the range of pure spontaneous emission has been left and the rate of stimulated emission reaches positive values.

Figure 4a shows time-integrated PL spectra taken from data matrices at different excitation densities normalized to peak A. We can see that:

- peak B grows out of the high energy tail of band A with increasing excitation. It becomes the main features of the spectra beyond densities of $32 \mu\text{J} \cdot \text{cm}^{-2}$, suggesting the presence of band filling.
- while the spectral position of peak B is almost excitation-independent, peak A shows an excitation-dependence, at low

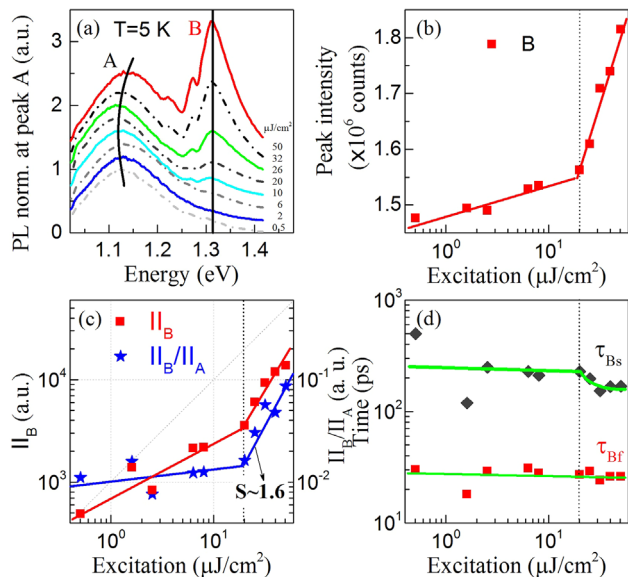


Figure 4. a) PL spectra taken from the TR-PL images at 1.5 ns versus excitation after being normalized to peak A. b) Excitation dependence of the intensity of peak B. c) Excitation dependence of the integral-intensity II of peak B, and the ratio of II_B/II_A . d) Excitation dependence of the fast and slow PL decay times of peak B. In (a), (b), and (d), the solid lines are guides to the eyes, and in (c) the solid lines are data fit curves.

powers a red-shift by ~ 25 meV, followed at $\sim 20 \mu\text{J} \cdot \text{cm}^{-2}$, by a blue-shift. This eliminates an increased lattice temperature as cause for the observed emission shifts.

Figure 4b shows the excitation dependence of the intensity of peak B. Very similar to the evolution of peak A derived from the decay curves in Figure 3d, peak B shows an even more pronounced superlinear behavior with the same threshold density of $\sim 20 \mu\text{J} \cdot \text{cm}^{-2}$, pointing to the value where the energy position of peak A turns from red- to blue-shift; see Figure 4a. An excitation dependence of the integrated intensity (II_B) is given in Figure 4c. In addition, the relative value of II_B normalized to peak A, the ratio of II_B/II_A , at different excitations, is plotted in Figure 4c. Beyond the threshold excitation density of $20 \mu\text{J} \cdot \text{cm}^{-2}$, it shows a superlinear increase ($S \approx 1.6$). Figure 4d gives the PL decay times of peak B. Notice that the background I_0 shows a linear evolution with excitation; see inset in Figure 3d. In concert with the superlinear behaviors of the intensity, the integral intensity and the ratio of II_B/II_A , peak B shows indication for ASE with a threshold value of $20 \mu\text{J} \cdot \text{cm}^{-2}$.

An interesting phenomenon should be pointed out that, when normalizing the PL decay data and blowing up the time scale toward the time resolution limits, the band B, i.e., the one at higher energies, appears delayed by $\Delta t \approx 8$ ps compared to band A, being spectrally located at lower photon energies. The value of Δt increases to 20 ps when the excitation decreases. In addition, the rise of both PL bands differs substantially. The steeper slope of band B demonstrates that the population of band B is much quicker than that of band A. This holds for different excitation levels. Details are shown in the Supporting Information.

Discussion: A variety of results is presented in the previous section. In the first place, our standard characterization provides

an image, which is very much consistent, with earlier findings for PbSe:Glass samples in the literature.^[1,35,36] This data is collected in Figure 1 and shows that our samples behave very similarly to those previously investigated by other researchers.

Our measurements at high excitation levels, however, provided a number of unexpected findings, in particular, if one compares our actual findings with those from an earlier study on highly excited PbS:Glass that was carried out with comparable methodology.^[14] There, we found stimulated emission located at almost the same spectral position, where the ground-state absorption peaked. Although the cw PL was 117 meV Stokes-shifted with respect to the ground-state absorption, the agreement was seen as strong evidence that we were actually observing stimulated emission from the ground-state in PbS:Glass. When looking to Figure 2d, we observe a 180 meV and 370 meV shift between ground-state absorption and bands A and B, respectively. Such a big shift can only be explained by the involvement of other states than ground-states. Therefore, we assign bands A and B to excited state emissions. For these states, we see a threshold like behavior (in several parameters) and a PL decay time reduction down to 40 and 25 ps for bands A and B, respectively, at high excitation levels. With the tentative assignment of bands A and B to ASE, we raise the question about the presence of ASE, or even stimulated emission, from the ground-state. However, such an emission, which should appear at a significantly lower threshold than the $\sim 20 \mu\text{J} \cdot \text{cm}^{-2}$ for bands A and B, was not observed. Of course, in this spectral range (~ 1.0 eV), there is a (weak) PL signal. However, there is absolutely no separate contribution, and the PL is only considered to be the low-energy shoulder of band A there. Even if this shoulder would contain a ground-state emission, we do not see any evidence of ASE in the kinetics.

We now address the absence of enhanced ground-state PL that is observed at the same time, when indications of ASE from excited states are seen. In InGaAs-based QD lasers,^[37,38] it was revealed that models, based on the analysis of rate equations as well as master equations,^[39] cannot adequately describe the features of QD laser behavior in presence of simultaneous emission from ground- and excited states. At the same time, two-state lasing has been observed, and quenching of the ground-state emission including stimulated and spontaneous emissions has been observed experimentally and by theoretical/numerical analysis.^[40,41] This means that a change from the ground- to excited-state emission is a standard situation in a QD laser, when excitation and/or temperature are increased. In our high-excitation experiment, the effective carrier temperatures are expected to be very high, as well. In addition, the 785-nm excitation photons (1.58 eV) are expected to populate excited states before the ground-states. Moreover, there could be optical loss mechanisms, which are more effective for ground-states. The experimental fact, however, is beyond any doubt, and clearly illustrated by Figure 2d. We can assume that at high excitation densities, in concert with a relatively high repetition rate result in strong carrier accumulation. Thus, the carriers prefer to stay at the excited states, the B and A bands, and satisfy the population inversion condition there.

There is another experimental fact, which should be addressed in brief. There is the delay between band A and B, where the lower-energy band A appears before the higher-energy

band B; see Figure S1a in the Supporting Information. Such a behavior cannot be understood within the frame of a common energy level scheme. However, the slopes of the onset of both decay curves increase with the excitation density; see Supporting Information Figure S1c. This could be related to a stimulated emission onset time.^[42] Simultaneously, the slope of band B decreases with temperature, while that of band A almost keeps constant; see Supporting Information Figure S1d. This suggests that the temperature mainly strengthens the exciton–phonon coupling of the higher band B and allows its carriers to relax more easily to the lower band A, but without any influence of the exciton–phonon coupling of band A.

Conclusion: We report the results of a study on the PL properties of PbSe:Glass at high optical excitation levels with the motivation to get to know the potential of the material as gain medium for laser applications. A basic characterization is made and shows that our samples represent the current standard of PbSe:Glass or PbS:Glass samples.

At high excitation levels, we see instead of the excitonic ground state emission, which is observed at low excitation levels with a PL decay time on the order of μs , at least two fast emission contributions energetically blue-shifted by up to 0.47 eV. For them, the initial PL decay time constant is $\sim 25\text{--}40$ ps. They are attributed to excited state emission. The presence of a superlinear increase in emission with a threshold of $\sim 20 \mu\text{J} \cdot \text{cm}^{-2}$ indicates the beginning of ASE. However, the absence of any emission from the ground state and a significantly higher threshold value compared to PbS:Glass indicate a poorer potential of PbSe:Glass as a gain medium compared to PbS:Glass.

All in all, our results indicate a rather complex situation. Although the ASE or even stimulated emission is observed from the excited states in PbSe:Glass, the absence of ground-state stimulated emission or ASE is in striking contrast to the situation in PbS:Glass.^[14] Probably this is due to a more flat shape of the density of states in PbSe:Glass compared to PbS:Glass. This makes ground-state lasing less likely and applications of PbSe:Glass as a laser material more difficult.

These statements are made on the basis of data from PbS:Glass samples, which provide clear indications of stimulated emissions.

Supporting Information

Supporting Information is available from the Wiley Online Library or from the author.

Acknowledgements

The authors thank Ms. R. J. Qi for the HR-TEM measurements. This work is supported by the National Key Research and Development Program (2016YFB0501604), and the Major Program (61790583) of the National Natural Science Foundation of China (61376103, 61275100).

Conflict of Interest

The authors declare no conflict of interest.

Keywords

amplified spontaneous emission, carrier accumulation, excited state emissions, PbSe quantum dots

Received: January 11, 2018

Revised: February 11, 2018

Published online:

- [1] F. W. Wise, *Acc. Chem. Res.* **2000**, *33*, 773.
- [2] G. Nootz, L. A. Padilha, P. D. Olszak, S. Webster, D. J. Hagan, E. W. Van Stryland, L. Levina, V. Sukhovatkin, L. Brzozowski, E. H. Sargent, *Nano Lett.* **2010**, *10*, 3577.
- [3] J. M. An, A. Franceschetti, S. V. Dudy, A. Zunger, *Nano Lett.* **2006**, *6*, 2728.
- [4] J. M. An, A. Franceschetti, A. Zunger, *Nano Lett.* **2007**, *7*, 2129.
- [5] I. Kang, F. W. Wise, *J. Opt. Soc. Am. B* **1997**, *14*, 1632.
- [6] S. Wageh, M. H. Badr, M. H. Khalil, A. S. Eid, *Physica E* **2009**, *41*, 1157.
- [7] E. U. Rafailov, M. A. Cataluna, W. Sibbett, *Nat. Photonics* **2007**, *1*, 395.
- [8] V. I. Klimov, *Science* **2000**, *290*, 314.
- [9] A. A. Mikhailovsky, A. V. Malko, J. A. Hollingsworth, M. G. Bawendi, V. I. Klimov, *Appl. Phys. Lett.* **2002**, *80*, 2380.
- [10] P. Landsberg, *Recombination in Semiconductors*. Cambridge University Press, Cambridge, UK **1991**.
- [11] R. D. Schaller, M. A. Petruska, V. I. Klimov, *J. Phys. Chem. B* **2003**, *107*, 13765.
- [12] L. Zhang, B. Zhang, S. Li, Q. Zhu, Y. J. Zheng, *Opt. Commun.* **2016**, *369*, 171.
- [13] A. R. Bahrapour, H. Rooholamini, L. Rahimi, A. A. Askari, *Opt. Commun.* **2009**, *282*, 4449.
- [14] F. Y. Yue, J. W. Tomm, D. Kruschke, P. Glas, *Laser Photonics Rev.* **2013**, *7*, L1.
- [15] N. F. Borrelli, D. W. Smith, *J. Non-Cryst. Solids* **1994**, *180*, 25.
- [16] F. Y. Yue, J. W. Tomm, D. Kruschke, P. Glas, K. A. Bzheumikhov, Z. C. Margushev, *Opt. Express* **2013**, *21*, 2287.
- [17] L. Cademartiri, E. Montanari, G. Calestani, A. Migliori, A. Guagliardi, G. A. Ozin, *J. Am. Chem. Soc.* **2006**, *128*, 10337.
- [18] I. Moreels, Z. Hens, *Small* **2008**, *4*, 3.
- [19] R. J. Ellingson, M. C. Beard, J. C. Johnson, P. Yu, O. I. Micic, A. J. Nozik, A. Shabaev, A. L. Efros, *Nano Lett.* **2005**, *5*, 865.
- [20] I. Moreels, Y. Justo, B. De Geyter, K. Haestraete, J. C. Martins, Z. Hens, *ACS Nano* **2011**, *5*.
- [21] I. Moreels, K. Lambert, D. Smeets, D. De Muyenck, T. Nolle, J. C. Martins, F. Vanhaecke, A. Vantomme, C. Delerue, G. Allan, Z. Hens, *ACS Nano* **2009**, *3*, 3023.
- [22] Y. P. Varshni, *Physica* **1967**, *34*, 149.
- [23] K. P. O'Donnell, X. Chen, *Appl. Phys. Lett.* **1991**, *58*, 2924.
- [24] F. Y. Yue, J. W. Tomm, D. Kruschke, B. Ullrich, J. H. Chu, *Appl. Phys. Lett.* **2015**, *107*, 022106.
- [25] A. Olkhovets, R. C. Hsu, A. Lipovskii, F. W. Wise, *Phys. Rev. Lett.* **1998**, *81*, 3539.
- [26] R. D. Schaller, J. M. Pietryga, S. V. Goupalov, M. A. Petruska, S. A. Ivanov, V. I. Klimov, *Phys. Rev. Lett.* **2005**, *95*, 196401.
- [27] J. Habinshuti, O. Kilian, O. Cristini-Robbe, A. Sashchiuk, A. Addad, S. Turrell, E. Lifshitz, B. Grandidier, L. Wirtz, *Phys. Rev. B* **2013**, *88*, 115313.
- [28] H. Du, C. L. Chen, R. Krishnan, T. D. Krauss, J. M. Harbold, F. W. Wise, M. G. Thomas, J. Silcox, *Nano Lett.* **2002**, *2*, 1321.
- [29] J. M. An, M. Califano, A. Franceschetti, A. Zunger, *J. Chem. Phys.* **2008**, *128*, 164720.

- [30] B. L. Wehrenberg, C. J. Wang, P. Guyot-Sionnest, *J. Phys. Chem. B* **2002**, *106*, 10634.
- [31] J. M. Luther, M. C. Beard, Q. Song, M. Law, R. J. Ellingson, A. J. Nozik, *Nano Lett.* **2007**, *7*, 1779.
- [32] G. Nair, S. M. Geyer, L. Y. Chang, M. G. Bawendi, *Phys. Rev. B* **2008**, *78*, 125325.
- [33] F. Y. Yue, J. W. Tomm, D. Kruschke, *Phys. Rev. B* **2013**, *87*, 195314.
- [34] F. Y. Yue, J. W. Tomm, D. Kruschke, *Phys. Rev. B* **2014**, *89*, 081303(R).
- [35] A. Lipovskii, E. Kolobkova, V. Petrikov, I. Kang, A. Olkhovets, T. Krauss, M. Thomas, J. Silcox, F. Wise, Q. Shen, S. Kycia, *Appl. Phys. Lett.* **1997**, *71*, 3406.
- [36] P. Dey, J. Paul, J. Bylsma, D. Karaiskaj, J. M. Luther, M. C. Beard, A. H. Romero, *Solid State Commun.* **2013**, *165*, 49.
- [37] V. V. Korenev, A. V. Savelyev, A. E. Zhukov, A. V. Omelchenko, M. V. Maximov, *Appl. Phys. Lett.* **2013**, *102*, 112101.
- [38] A. E. Zhukova, M. V. Maximov, Y. M. Shernyakov, D. A. Livshits, A. V. Savelyev, F. I. Zubov, V. V. Klimenko, *Semiconductors* **2012**, *46*, 231.
- [39] A. Markus, A. Fiore, *Phys. Status Solidi A* **2004**, *201*, 338.
- [40] M. Gioannini, *J. Appl. Phys.* **2012**, *111*, 043108.
- [41] A. Röhm, B. Lingnau, K. Ludge, *IEEE J. Quantum Electron.* **2015**, *51*, 2000211.
- [42] J. K. Song, U. Willer, J. M. Szarko, S. R. Leone, S. Li, Y. Zhao, *J. Phys. Chem. C* **2008**, *112*, 1679.